Brief Reports

Brief Reports are short papers which report on completed research which, while meeting the usual **Physical Review** *standards of scientific quality, does not warrant a regular article. (Addenda to papers previously published in the* **Physical Review** *by the same authors are included in Brief Reports.) A Brief Report may be no longer than 3½ printed pages and must be accompanied by an abstract. The same publication schedule as for regular articles is followed, and page proofs are sent to authors.*

New photoelectron spectroscopic procedure for the precise location of the edges of electron energy bands

B. Craig Meyers and T. E. Feuchtwang
Department of Physics, The Pennsylvania State University, University Park, Pennsylvania 16802
(Received 21 March 1983)

An analysis of band-gap emission is presented for a semi-infinite Kronig-Penney model. The results suggest that singularities predicted for the energy derivative of the angle-resolved energy distribution may provide an accurate method to identify the edges of both initial (occupied) and final (unoccupied) energy bands of the photoemitter.

I. INTRODUCTION

The emission of a photoelectron which has been excited from an initial state to a final state whose energy E_f lies in a forbidden gap of the infinite solid, located above the vacuum level, is known as "band-gap" photoemission. The ability to experimentally detect and identify such photoelectrons is important for several reasons. In particular, these electrons may be expected to be sensitive to band edges and provide a precise experimental determination of the band edges which would be useful to assess theoretically calculated band structures. It is the purpose of this paper to propose a method which may provide such a determination of the edges of both initial- and final-state energy bands by observing discontinuities or singularities in the energy derivative of the angle-resolved energy distribution $d^3j/d\Omega\, d^2E_f$.

This paper is organized as follows: in the next section a description of the semi-infinite Kronig-Penney model is given as well as a brief discussion of the procedure used to calculate the final state of the photoelectron in vacuum. The results are used to calculate band-gap photoemission and to identify the band edges which are discussed in Sec. III. Our conclusions are summarized in Sec. IV. Further details of the calculation will be published separately.[1]

II. MODEL DESCRIPTION AND SOLUTION

A. Model description

The calculation of band-gap photoemission is based on a semi-infinite, or modified, Kronig-Penney (KP) model whose potential $V(\vec{r})$ is defined by

$$V(\vec{r}) \equiv V(z) = \begin{cases} 0, & z > 0 \\ \dfrac{\hbar^2}{2m}\dfrac{2P}{a}\displaystyle\sum_{n=0}^{\infty}\delta(z+na+b), & z < 0 \end{cases} . \tag{1}$$

In the above, the lattice constant is a, the location of the surface plane is b, and the dimensionless strength of the potential is P. The values of these parameters were chosen to be 5.65, 0.0, and 0.30 a.u., respectively. These values are characteristic of Na, for which the Fermi energy $E_F = 3.24$ eV, the work functions is 2.30 eV, and the plasma energy $\hbar\omega_p = 5.75$ eV. The potential defined by Eq. (1) was used by Schaich and Ashcroft[2] (SA) in their analysis of photoemission from a semi-infinite solid.

The dispersion relation which determines k, the z component of the (complex) wave vector $\vec{K} = (\vec{K}_\rho, k)$ as a function of the "normal" energy $\tilde{E} = E - \hbar^2 K_\rho^2/2m$ is given by[2]

$$\cos(ka) = \cos(\tilde{k}a) + \frac{P\sin(\tilde{k}a)}{\tilde{k}a}; \quad \tilde{k} = \frac{1}{\hbar}(2m\tilde{E})^{1/2} . \tag{2}$$

B. Calculation of the photoemitted final state

The final state of the photoemitted electron is calculated using the scattering formalism developed by Adawi,[3] i.e.,

$$\Psi_f(\vec{r}, E+\hbar\omega) = \int_{-\infty}^{\infty} G_0(\vec{r}, \vec{r}'; E+\hbar\omega)\mathcal{V}'(\vec{r}') \times \Phi_0(\vec{r}', E)\, d\vec{r}' . \tag{3}$$

In the above, $G_0(\vec{r}, \vec{r}'; E+\hbar\omega)$ is the Green function for the electronic Hamiltonian, in the absence of the radiation field, at the energy $E+\hbar\omega$. Since the potential $V(\vec{r})$ is separable we may consider a "reduced" Hamiltonian which involves only the normal, or z, coordinate. In this case, the Green function may be constructed using the Wronskian technique[4] in terms of the eigenfunctions of the modified KP model, which are easily determined.[2,5] We have accounted for an assumed finite extraction length L of the photoexcited electrons by including a factor $\exp(Lz)$ in the unperturbed final state. A similar procedure was followed by SA in their discussion of photoemission from the modified KP model.[2] The initial state of the electron is denoted $\Phi_0(\vec{r}, E)$.

In Eq. (3) the perturbation due to the incident photons is described by the interaction

$$\mathcal{H}' = \frac{e}{mc}\vec{A}(\vec{r})\cdot\vec{p} \ , \tag{4}$$

where $\vec{p}$ is the electron momentum operator and the vector potential is denoted by $\vec{A}(\vec{r})$. For the problem at hand we have chosen to represent the vector potential in the formalism of Melnyk and Harrison[6]; thus,

$$\vec{A}(\vec{r}) = \begin{cases} \hat{\epsilon}_T a_0 T \exp[-i(\vec{Q}_\rho\cdot\vec{\rho}+q_T z)] + \hat{\epsilon}_L a_0 L \exp[-i(\vec{Q}_\rho\cdot\vec{\rho}+q_L z)], & z<0 \\ \hat{\epsilon}_I a_0 \exp[-i(\vec{Q}_\rho\cdot\vec{\rho}+qz)] + \hat{\epsilon}_R a_0 R \exp[-i(\vec{Q}_\rho\cdot\vec{\rho}-qz)], & z>0 \ . \end{cases} \tag{5}$$

In Eq. (5) the amplitudes of the incident, reflected, transverse, and longitudinal fields are denoted by a_0, a_0R, a_0T, and a_0L, respectively. Similarly, the wave vectors for the incident, reflected, transverse, and longitudinal fields are, respectively, denoted by $\vec{Q}_I=(\vec{Q}_\rho,q)$, $\vec{Q}_R=(\vec{Q}_\rho,-q)$, $\vec{Q}_T=(\vec{Q}_\rho,q_T)$, and $\vec{Q}_L=(\vec{Q}_\rho,q_L)$. The model is assumed to be translationally invariant in the directions parallel to the surface. Consequently, $\vec{Q}_\rho$, the two-dimensional component of the photon wave vector parallel to the surface is conserved in the scattering at the surface. Although we have explicitly accounted for the longitudinal field, for the range of photon energies considered, namely, $\hbar\omega \gtrsim 3F_F$, the contribution of the longitudinal field is negligible.[7]

The photoemitted current density $\vec{j}$ in the state Ψ_f is of the form

$$\vec{j}(\hbar\omega) = \hat{z}j(\hbar\omega) \ , \tag{6a}$$

where

$$j(\hbar\omega) = \frac{2}{(2\pi)^3}\frac{e\hbar}{m}\cos^2\theta_p \int\left(\frac{2mE_f}{\hbar^2}\right)^{3/2}\cos^2\theta|M|^2\frac{dk_i}{dE_i}d\Omega\, dE_f \ . \tag{6b}$$

In Eq. (6b) the integration with respect to the solid angle extends only over the hemisphere $0\leq\theta\leq\pi/2$. M is the relevant transition "matrix element." The angular position of the detector relative to the surface normal is denoted by θ, and θ_p is the photon angle of incidence. The angle-resolved energy distribution curve (AREDC) at constant photon energy is

$$\left.\frac{d^2j(E_f)}{d\Omega\, dE_f}\right|_{\hbar\omega=\text{const}} = \frac{2}{(2\pi)^3}\frac{e\hbar}{m}\cos^2\theta_p\left(\frac{2mE_f}{\hbar^2}\right)^{3/2}\cos^2\theta|M|^2\left.\frac{dk_i}{dE}\right|_{E=E_f-\hbar\omega} \ . \tag{7a}$$

The AREDC at constant-initial-state (CIS) energy is

$$\left.\frac{d^2j(\hbar\omega)}{d\Omega\, dE_f}\right|_{\substack{E_i=\text{const.}\\ E_f=E_i+\hbar\omega}} = \frac{2}{(2\pi)^3}\frac{e\hbar}{m}\cos^2\theta_p\left(\frac{2mE_f}{\hbar^2}\right)^{3/2}\cos^2\theta|M|^2\left.\frac{dk_i}{dE}\right|_{E=E_i=\text{const}} \ , \tag{7b}$$

and a similar expression defines the AREDC at constant-final-state (CFS) energy. Finally, we note that the AREDC is a function of both E_f and k_f^{in}, where k_f^{in} is the normal or z component of the final wave vector of the electron inside the metal. Hence the energy derivative of the AREDC can be written in the form

$$\frac{d^3j(\hbar\omega;E_f,k_f)}{d\Omega\, d^2E_f} = \frac{\partial}{\partial E_f}\left(\frac{d^2j}{d\Omega\, dE_f}\right) + \frac{\partial}{\partial k_f^{\text{in}}}\left(\frac{d^2j}{d\Omega\, dE_f}\right)\frac{dk_f^{\text{in}}}{dE_f} \ . \tag{8}$$

III. RESULTS AND DISCUSSION

We shall now present results illustrating band-gap photoemission from the modified KP model. These results were obtained for a "normal-emission constant-initial-state" (NECIS) experimental configuration. That is, we assumed the electron detector to be located on the normal to the surface, and that the energy accepted by the detector is swept together with the photon energy, thus keeping the initial electron energy constant. Such an experiment scans over final electron energies and was used by Feuerbacher and Christensen[8] in their analysis of band-gap emission from W(110).

In Fig. 1 we present NECIS results for an initial electron energy $E_i=-5.32$ eV as a function of the extraction length L. This initial energy corresponds to an initial wave vector $k_i\simeq 0$. The photon angle of incidence was 30° and the photon energy varied from 16.0 to 18.0 eV.[9]

The range of photon energies over which band-gap emission occurs is indicated in Fig. 1 by a horizontal arrow. We shall show that the AREDC exhibits discontinuities in slope at both edges of the forbidden gap. The peaks in the emission intensity, which become prominent at larger extraction lengths, occur for $L/a\gtrsim 10$ at photon energies $\hbar\omega=16.3$ and 17.3 eV. These correspond to L/a-independent direct transition energies for electrons photoexcited from the initial state of energy E_i to the lower (d_l) and upper (d_u) final energy bands, respectively. We note that the intensity of the band-gap emission is comparable to the intensity of emission from the adjacent allowed (final) bands. As expected, our calculations indicate an increased emission intensity from the band gap when the initial state is located near a Brillouin-zone boundary. This effect can be traced to the factor dk_i/dE, in Eqs. (7), which diverges at a zone boundary. In a real solid this effect may also occur at a critical point or over a flat region of the band structure located inside the Brillouin zone, i.e., whenever $dk_{z,i}/dE$ diverges.

An analysis of Fig. 1 suggests that the edges of the forbidden gap may be identified with structure in the AREDC. However, a more accurate determination of the band edges may be obtained by a differentiation of the AREDC with respect to the final electron energy. The differentiated

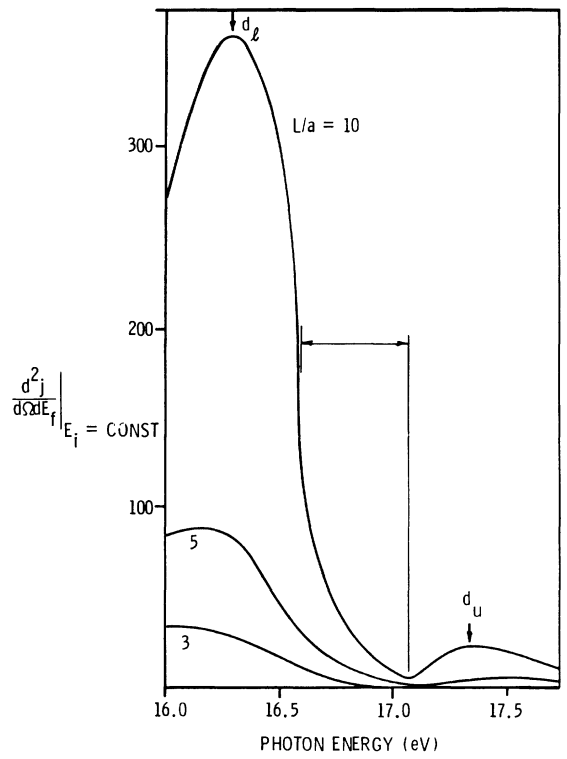

FIG. 1. Normal-emission constant-initial-state (NECIS) spectrum $d^2j/d\Omega\, dE_F|_{E_i=\text{const},\,\theta=0}$ for an initial energy $E_i = -5.32$ eV as a function of extraction length L. The range of photon energies for which band-gap emission occurs is indicated by an arrow. Photon energies corresponding to direct transitions to a final state in the lower and upper energy bands are denoted by d_l and d_u, respectively.

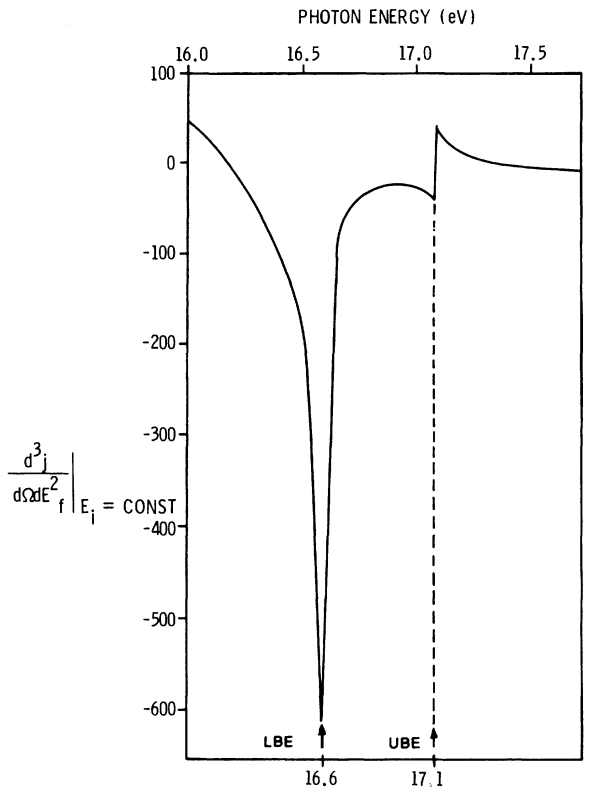

FIG. 2. Derivative of NECIS spectrum with respect to final electron energy $d^3j/d\Omega\, dE_f^2|_{E_i=\text{const},\,\theta=0}$ for extraction length $L = 5a$. The edges of the lower and upper final bands are denoted by LBE and UBE, respectively. The dashed line illustrates the expected result for $d^3j/d\Omega\, dE_f^2$ at the upper band edge which would be obtained using a finer mesh in the vicinity of the band edge.

AREDC is presented in Fig. 2 for an extraction length $L = 5a$. Calculations using other values of L indicate that the shape of $d^3j/d\Omega\, d^2E_f$ is essentially independent of the extraction length. The differentiated spectrum presented in Fig. 2, exhibits sharp negative peaks or singularities at the (upper) edge of the lower band (LBE), i.e., $\hbar\omega = 16.6$ eV, and at (lower) edge of the upper band (UBE), i.e., $\hbar\omega = 17.1$ eV. The singularities of the differentiated AREDC can be explained in terms of the band structure and the matrix element for photoemission.

The occurrence of singularities in the AREDC at the band edges may be understood in terms of Eq. (8), specialized to the present experimental configuration. Specifically at the edges of the final energy bands the factor dk_f^{in}/dE_f becomes singular.

The nature of the singularities in the AREDC is determined by the matrix element. Namely, due to the continuing decrease in electron emission as the final electron energy $E_f = E_i + \hbar\omega$ sweeps across the LBE into the forbidden energy gap, we expect a *negative infinite slope* at the LBE. This implies that the AREDC exhibits at the LBE an inflection point and a vertical tangent. On the other hand, we expect a *vertical cusp* at the UBE due to the sign reversal of the infinite slope at this gap edge. This sign reversal is a matrix element effect which reflects the increase in the AREDC as the photon energy appropriate for the direct transition, d_u, from E_i is approached from below. For $L/a \gtrsim 10$, d_u corresponds to a local maximum of AREDC. Figure 2 indicates that the positive slope of the AREDC decreases from the UBE, and that for $L/a = 5$, this slope vanishes at a photon energy definitely above d_u. However, the vertical cusp at the UBE is not resolved in Fig. 1, where it is marked by an apparent minimum in the AREDC.

It should be emphasized that the occurrence of singularities in the differentiated AREDC per se, being a band-structure effect, is not affected by the (matrix element determined) presence or absence of direct transitions from the particular initial state involved in the NECIS experiment; only their detailed structure is.

Equation (8) also predicts that, due to the presence of the singular factor dk_f^{in}/dE_f, the identification of the extrema of the band structure in the differential NECIS spectrum should be much less sensitive to the extraction length than their identification in the NECIS spectrum itself. This prediction is confirmed by the comparison of Fig. 2 and the spectra for $L = 5a$ and $10a$ in Fig. 1. Figure 2 clearly indicates that at the LBE the spectrum for $L = 5a$ should exhibit the vertical tangent which characterizes the bulk band structure. However, this is not confirmed by Fig. 1; the spectrum for $L = 10a$ exhibits the expected vertical tangent, in contrast to the spectrum for $L = 5a$, which does not exhibit any special feature at the LBE. The preceding discussion suggests that the *observation of singularities in the derivative of the AREDC may provide a more accurate experimental determination of the extrema of energy bands than the AREDC.*

Finally, we note an interesting point: although the KP

energy bands are symmetric with respect to the middle of the band gap, which in Fig. 2 occurs at $\hbar\omega = 16.85$ eV, neither the AREDC nor its derivative exhibit this symmetry. This absence of symmetry is a matrix element effect. Specifically, it is due to the first term on the right-hand side of Eq. (8). That is, the explicit dependence of the AREDC on the final electron energy, as opposed to its implicit energy dependence, is responsible for the asymmetry. Furthermore, the presence of the term $(\partial/\partial E_f)(d^2j/d\Omega\, dE_f)$ complicates the interpretation of $d^3j/d\Omega\, dE_f^2$ in terms of the complex band structure, because this quantity is evidently not simply proportional to the density of states $|\nabla_k E_f|^{-1}$.

The preceding results illustrate that NECIS spectroscopy may provide a technique for the accurate determination of band edges for excited-state bands. Similarly, the use of constant–final-state (CFS) spectroscopy is expected to be useful for the identification of the edges of initial energy bands. Here it should be noted that dipole transition selection rules[10,11] may exclude the observation of certain final band edges in NECIS due to the symmetry of the corresponding states.

IV. CONCLUSIONS

An analysis of band-gap photoemission from a modified Kronig-Penney model has been presented. The explicit analysis is clearly model dependent; however, we expect its qualitative predictions to be generally applicable. Specifically, this calculation predicts singularities or discontinuities in the energy derivative of the AREDC observed in "normal-emission constant–initial-state spectroscopy." It is suggested that this may provide an accurate identification of the extrema of (final) excited bands. Similarly, "constant–final-state spectroscopy" may be expected to allow a corresponding determination of extrema of (initial) occupied bands.

It should be noted that while our anlaysis was in terms of $d^3j/d\Omega\, dE_f^2$, similar results would be obtained in terms of $d^3j/d\Omega\, dE_f\, d(\hbar\omega)$. Experimentally, the derivative of the AREDC with respect to photon energy is expected to provide more accurate results, especially when synchrotron radiation is available. Finally, it is interesting to note that while band-gap emission is generally believed to be a surface-sensitive phenomenon, it evidently also carries information about the bulk band structure.

ACKNOWLEDGMENTS

This research was supported in part by the Applied Research Laboratory of The Pennsylvania State University, Grant No. E/F 6161.

[1]B. C. Meyers and T. E. Feuchtwang (unpublished).
[2]W. L. Schaich and N. W. Ashcroft, Phys. Rev. B 3, 2452 (1971).
[3]I. Adawi, Phys. Rev. 134, A788 (1964).
[4]See, for example, P. M. Morse and H. Feshbach, *Methods of Theoretical Physics* (McGraw-Hill, New York, 1953), Vol. 1, p. 832.
[5](a) M. Sachs, *Solid State Theory* (McGraw-Hill, New York, 1963), p. 193; (b) C. Kittel, *Introduction to Solid State Physics*, 5th ed. (Wiley, New York, 1976), p. 191.
[6]A. R. Melnyk and M. J. Harrison, Phys. Rev. B 2, 835, 851 (1970).
[7]For a justification of this statement see B. C. Meyers and T. E. Feuchtwang, Phys. Rev. B 27, 2030 (1983).
[8]B. Feuerbacher and N. E. Christensen, Phys. Rev. B 10, 2373 (1974); N. E. Christensen and B. Feuerbacher, *ibid.* 10, 2349 (1974).
[9]It is to be noted that the amplitudes R, T, and L defined in Eq. (5), are photon energy dependent. We have, however, used the values for $\hbar\omega = 16$ eV. This value satisfies the constraint $\hbar\omega > 3E_F$ and the dependence of the field amplitudes on photon energy is expected to be small for small fractional changes in photon energy. This will not be the case for smaller photon energies, particularly those near the plasma energy $\hbar\omega_p$.
[10]J. Hermanson, Solid State Commun. 22, 9 (1977).
[11]W. Eberhadt and F. J. Himpsel, Phys. Rev. B 21, 5572 (1980).